Deriving Reaction Mechanisms from Kinetic Spectroscopy. Application to Late Rhodopsin Intermediates

I. Szundi, J. W. Lewis, and D. S. Kliger
Department of Chemistry and Biochemistry, University of California, Santa Cruz, California 95064 USA

ABSTRACT A general algebraic approach to the kinetic analysis of time-dependent absorption data is presented that allows the calculation of possible kinetic schemes. The kinetic matrices of all possible reaction mechanisms are calculated from experimental eigenvalues and eigenvectors derived from the decay constants and amplitude spectra (b-spectra) of the global exponential fit to the time-dependence of the absorption data. The eigenvalues are directly related to the decay constants, and the eigenvectors are obtained by decomposing the b-spectra into spectral components representing the intermediates. The analysis method is applied to the late intermediates (lumi, meta I, meta I-380, and meta II) of the rhodopsin photoreaction. The b-spectra are decomposed into lumi, meta I, meta-380, and rhodopsin spectra. The meta-380 component is partitioned into isospectral meta I-380 and meta II components based on physical criteria. The calculated kinetic matrices yield a number of reaction mechanisms (linear scheme with back reactions, branched schemes with equilibrium steps, and a variety of square models) consistent with the photolysis data at 25°C. The problems associated with isospectral intermediates (meta I-380 and meta II) are treated successfully with this method.

INTRODUCTION

Advances in time-resolved optical spectroscopy instrumentation have provided data at a rate that challenges analysis techniques. Although very general matrix methods have been developed to characterize these data numerically (Hofrichter et al., 1983) and analyze these data in terms of presumed schemes (Henry, 1997), analysis of the numerical results (apparent rates and the spectral changes associated with them) to deduce chemical mechanisms has proven to be more difficult. Approaches tend to be individualized to specific molecular systems (Parkhurst, 1979; Linschitz and Kasche, 1966; Chen et al., 1996) and are difficult to generalize. Among the retinal proteins, bacteriorhodopsin served as a model system for both structural and photochemical studies. There has been a continuous effort to develop rigorous and general analysis methods based on solid mathematical foundations (Nagle, 1991; Lozier et al., 1992; Nagle et al., 1995) to describe the photocycle kinetics of this protein. The methods rely almost exclusively on information from the time domain and make extensive use of the time-dependence of intermediate concentrations. These can only be obtained for the most thoroughly studied systems, such as bacteriorhodopsin, and even there with some uncertainty. Because of limitations in instrumentation and computational power, previous approaches to molecular schemes have been based on intuitive, or random, guesses, and used mathematical techniques that merely confirm one or the other presumed scheme. Technological advances have overcome these problems, allowing all possible chemical mechanisms to be tested, but such testing still remains a difficult task in the absence of a systematic approach.

Here we give a general approach to finding kinetic schemes applicable to first-order or pseudo-first-order reaction mechanisms. A major advantage of this method, as presented here, is that the intermediate results can be interpreted in chemical terms, removing the ad hoc character of some fitting methods. Our approach also can deal with isochromic intermediate spectra that have been proposed to occur in bacteriorhodopsin (Varo and Lanyi, 1991) and rhodopsin (Hofmann, 1986; Straume et al., 1990; Thorgeirsson et al., 1992). As an example we apply the technique to photolysis data for membrane suspensions of bovine rhodopsin recorded in the microsecond-to-millisecond time window at room temperature. In that system the method finds new mechanisms capable of fitting the data. This gives confidence that all possible mechanisms have been considered when additional physical criteria are subsequently applied to isolate a unique mechanism.

THEORY

General strategies to derive kinetic schemes

The majority of photochemical reactions involving proteins are intramolecular conversions and belong to the class of first-order or pseudo-first-order reaction mechanisms. The most difficult and controversial step in the kinetic analysis is the derivation of the kinetic scheme. A good scheme not only describes the experimental data adequately, but also contains reaction rate constants that follow the Arrhenius law and yields acceptable absorption spectra of the intermediates. There are excellent reviews on this topic (Lozier et al., 1992; Nagle et al., 1995). Therefore, we give only a short overview of the problem and outline the main strategies commonly used in its solution.

Received for publication 3 February 1997 and in final form 2 May 1997.
Address reprint requests to Dr. David S. Kliger, Dept. of Chemistry and Biochemistry, University of California at Santa Cruz, Santa Cruz, CA 95064. Tel.: 408-459-2106; Fax: 408-459-4161; E-mail: kliger@chemistry.ucsc.edu.

0006-3495/97/08/688/15 $2.00

In the kinetic studies of intramolecular photoconversions of chromoproteins the concentrations of the intermediates are not measured directly; rather, the time-dependence of the absorption spectrum of the system is most often recorded. The absorption spectrum at time t is the sum of absorbances of all the components present in the system:

$$\boldsymbol{a}(\lambda, t) = \epsilon(\lambda)\, \boldsymbol{c}(t) \tag{1}$$

where $\epsilon(\lambda)$ is a matrix whose columns are the extinction coefficients of the intermediates at the given set of wavelengths, λ, and $\boldsymbol{c}(t)$ is a vector containing the time-dependent concentrations of the intermediates. The concentration vector can be obtained by integration of the differential equations describing the reactions in the scheme, and for the first-order reactions we are discussing here it is a sum of exponentials. The working equation of the kinetic analysis becomes:

$$\boldsymbol{a}(\lambda, t) = \epsilon(\lambda) \sum_i \boldsymbol{c}_{0i} \exp(-r_i\, t) \tag{2}$$

where the exponents r_i are the apparent rate constants and $\boldsymbol{c}_{0i}$ are the preexponential factors, both being combinations of the microscopic rate constants corresponding to the individual steps in the reaction scheme.

The ultimate goal of the kinetic analysis is to derive the kinetic scheme and the absorption spectra of all the components in the system. The microscopic rate constants have to be obtained from the apparent rates determined experimentally, and this can only be done for a few simple schemes, namely when the number of individual steps in a kinetic scheme does not exceed the number of apparent rate constants. The unidirectional sequential scheme without back reactions is a useful example. In many instances these simple schemes do not yield acceptable intermediate spectra, and reaction schemes with more individual steps are needed. At this point a major problem arises, because it appears that Eq. 2 is underdetermined for all but a few simple kinetic schemes. This difficulty can be overcome and the working equation can be solved, in theory, for an extended data set that combines measurements taken under different conditions, such as at different temperatures. It is assumed that the intermediate spectra remain unchanged and the microscopic rate constants follow the Arrhenius law. However, this general approach is difficult in practice because of the immense computational difficulties and the uncertainty of the results due to the limited accuracy of experimental data.

All practical approaches aimed at the solution of the underdetermined kinetic problem incorporate the following general rule: of the many possible solutions, only those are selected that provide microscopic rate constants following the Arrhenius law and yield temperature-invariant intermediate spectra of defined shapes. Although there are many different strategies used, which we do not intend to review individually, they can be classified into two categories.

1) In the most common strategy the analysis starts with the assumption of the kinetic scheme with microscopic rate constants adjusted to yield the experimental apparent rate constants. It is followed by the calculation of the time dependence of the concentration vector, and it is completed with the calculation of the intermediate spectra from the concentration values and the experimental absorbance data using Eq. 1. The scheme is judged by the quality of the derived intermediate spectra. This method of analysis suffers from the lack of a straightforward relationship between the values of the microscopic rate constants entered in the first step and the shape of the intermediate spectra emerging from the last step of the calculation.

2) The second strategy makes use of the fact that any proposed kinetic scheme is finally judged by the quality of the intermediate spectra it produces. The analysis starts with the definition of a set of intermediate spectra and follows with the calculation of the concentration time dependence from the experimental absorption data using Eq. 1. The time dependence is then fit to a variety of kinetic schemes and the most appropriate ones are chosen. The advantage of this approach over the previous one lies in the relatively straightforward relationships that connect the concentration profiles with the kinetic schemes. The intermediate spectra needed in this approach are commonly imported from absorbance measurements taken at low temperatures or under special circumstances when intermediates can be trapped. In theory, Eq. 1 yields the correct concentration profile. In practice, however, it is not always so. Intermediates with heavily overlapping spectral shapes are difficult to separate and the calculated concentration time dependence may contain a mixture of intermediates. Any misjudgments and errors in the intermediate spectra may have severe consequences for the final results.

The common feature of the two analysis strategies is that the search for the proper kinetic scheme(s) is ad hoc. The strategies provide very little, if any, guidance and clues regarding the possible steps in the kinetic scheme, and it is almost impossible to decide whether all reasonable schemes have been tried. The mathematical methods involved in the search for the kinetic scheme are mechanistic, repetitive fitting procedures with very little, if any, opportunities for interactions from the user side.

We propose a different approach for the analysis of kinetic data, which starts with the assumption of the intermediate spectra, just like the second strategy above. However, its logic and the mathematical tools it uses are significantly different. The method furnishes many clues to recognize the main elements of the possible schemes from visual observation of the experimental data, and allows the user to incorporate and test intuitive guesses regarding the shape of the intermediate spectra and the structure of the kinetic scheme. The most important new feature of the method is that it allows the calculation of the kinetic scheme from intermediate components obtained by decomposing the experimental b-spectra (the difference spectra associated with the observed rates) with reasonable accuracy. The

calculated scheme is either a simple one, or, in more complex situations, it contains a combination of the possible kinetic pathways that will end up in one or more schemes after simplifications. The mathematical tools used in our approach can also be used to evaluate kinetic schemes suggested previously but that heretofore lacked rigorous tests.

The method of derivation of kinetic schemes from analysis of b-spectra

The method is based on linear algebra and makes extensive use of the connections between the steps in the kinetic scheme and the components of the eigenvectors of the kinetic matrix. The eigenvectors will be extracted from b-spectra obtained in a global exponential fit to the experimental data. Below we describe the mathematical basis of the technique.

Description of absorption kinetics

In the mathematical treatment of absorption kinetics we follow the algebraic methods discussed by Thorgeirsson et al. (1993). The reaction scheme involving n intermediates is described by a set of first-order differential equations:

$$\boldsymbol{c}(t)' = \boldsymbol{K}\,\boldsymbol{c}(t); \tag{3}$$

where $\boldsymbol{c}(t)$ is the concentration column vector of length n, $\boldsymbol{c}(t)'$ is its time derivative, and $\boldsymbol{K}$ is the kinetic matrix. The kinetic matrix is an $n \times n$ matrix composed of the microscopic rate constants, k_{ij}, which describe the conversions from intermediates i to j. The elements of the kinetic matrix are as follows: $K_{ji} = k_{ij}$ when $i \neq j$, and $K_{ii} = -\Sigma_j k_{ij}$ for the diagonal elements. The general solution to the set of differential equations is a sum of exponentials of the form:

$$\boldsymbol{c}(t) = \sum_i \boldsymbol{p}_i \exp(\alpha_i\, t). \tag{4}$$

For a few degenerate systems, e.g., sequential schemes with identical microscopic rates, the general solution is more complicated. However, their occurrence in practice is rare. The exponents α_i are the eigenvalues of the kinetic matrix, and the preexponential factors $\boldsymbol{p}_i$ are related to its eigenvectors, $\boldsymbol{v}_i$:

$$\boldsymbol{p}_i = f_i\,\boldsymbol{v}_i \tag{5}$$

where f_i is a scalar factor obtained from the initial conditions, i.e., from the concentration vector at zero time. Because of the mass conservation law, the kinetic matrix is singular and one of its eigenvalues is zero. The corresponding eigenvector, $\boldsymbol{v}_0$, describes a time-independent state. The absorption spectrum and the concentration vector at any given time are related by the formula:

$$\boldsymbol{a}(\lambda, t) = \epsilon(\lambda)\boldsymbol{c}(t) \tag{6}$$

where $\epsilon(\lambda)$ is a matrix of the extinction coefficients of the intermediates. In practice, absorption difference spectra are measured; therefore, the spectrum of the missing bleached form should be subtracted from the absolute spectra given by Eq. 6. Combining Eqs. 4–6 above, the final formula describing the time-dependent absorption changes, $\Delta\boldsymbol{a}(\lambda, t)$, can be written as:

$$\Delta\boldsymbol{a}(\lambda, t) = \epsilon(\lambda)\left(\sum_i f_i\,\boldsymbol{v}_i \exp(\alpha_i\, t) - \boldsymbol{c}_{bl}\right) \tag{7}$$

where $\boldsymbol{c}_{bl}$ is the concentration vector of the photolysed (bleached) components.

In global exponential fitting the time dependence of the absorption difference spectra is fitted to a sum of exponentials of the following form:

$$\Delta\boldsymbol{a}(\lambda, t) = \sum_i \boldsymbol{b}_i(\lambda)\exp(-r_i\, t) + \boldsymbol{b}_0(\lambda). \tag{8}$$

The exponents r_i are the experimental decay constants, also called apparent rate constants, and the amplitudes of the time-dependent $\boldsymbol{b}_i(\lambda)$, and time-independent $\boldsymbol{b}_0(\lambda)$, components are referred to as b-spectra. Comparing Eq. 7 with the form of the global fit, Eq. 8, one can easily see that b-spectra are linear combinations of intermediate spectra:

$$\boldsymbol{b}_i = \epsilon(\lambda) f_i\,\boldsymbol{v}_i \tag{9}$$

for nonzero eigenvalues, and

$$\boldsymbol{b}_0 = \epsilon(\lambda)(f_0\,\boldsymbol{v}_0 - \boldsymbol{c}_{bl}) \tag{10}$$

for the time-independent state. Notice that the b_0-spectrum represents the difference between the spectra of the final photoproduct, denoted by the time-independent concentration vector, $f_0\,\boldsymbol{v}_0$, and the initial pigment, $\boldsymbol{c}_{bl}$. For a cyclic process the b_0-spectrum becomes zero because the final photoproduct is the recovered material that has been previously photolysed. The components of the scaled eigenvectors represent the contributions of each intermediate to that particular b-spectrum. We will use the latter relationships extensively in our attempts to deduce kinetic schemes.

Reconstruction of eigenvectors from b-spectra

To reconstruct the eigenvectors we will decompose the experimental b-spectra into individual components of defined spectral shapes and relative amplitudes. The spectral shapes will be dealt with later. Here we discuss the balance equations that apply to the matrix of eigenvectors.

The first equation is the balance of amplitudes within each b-spectrum, which can be derived in the following way. Because of the mass conservation law, the sum of the components of the concentration vector should yield the total amount of the bleached material at any time:

$$\sum_j c_{blj} = \sum_j c_j = \sum_j \sum_i f_i\, v_{ji} \exp(-\alpha_i\, t) \tag{11}$$

The right-hand side of Eq. 11 can be separated into terms corresponding to nonzero and zero eigenvalues. At infinite time only the term corresponding to the zero eigenvalue remains:

$$\sum_j c_{bl} = \sum_j f_0 \, v_{j0} \tag{12}$$

By comparing Eqs. 11 and 12 it is easy to see that

$$\sum_j v_{ji} = 0 \tag{13}$$

for all b-spectra that correspond to nonzero decay constants. Because we measure absorption difference spectra the balance equation also holds for the decomposition of the time-independent experimental b-spectrum, as it contains the concentration vector of the bleached material as a negative term (see Eq. 10).

The second condition the eigenvectors from b-spectra decomposition should satisfy is the balance of amplitudes for each intermediate, that is, the balance among b-spectra. By setting the time to zero in Eq. 4 we can write the balance equation:

$$\sum_i f_i \, v_{ji} = c_j(t = 0) \tag{14}$$

The concentration vector in this equation contains zero for each intermediate that is not present at zero time. Eq. 14 has two useful practical applications. First, it can be used to find out which intermediates are present at zero time; that is, in the first recorded spectrum, and second, it shows that intermediates appearing during the photoreactions should be present in more than one of the b-spectra.

Calculation of the kinetic matrix from experimental eigenvectors and eigenvalues

It is known from linear algebra that an $n \times n$ matrix $\boldsymbol{K}$ that has n independent eigenvectors can be diagonalized by the $n \times n$ eigenvector matrix $\boldsymbol{V}$ constructed from them:

$$\boldsymbol{\alpha} = \boldsymbol{V}^{-1} \boldsymbol{K} \boldsymbol{V}. \tag{15}$$

The elements of the diagonal matrix, α, thus produced are the eigenvalues of $\boldsymbol{K}$. Conversely, by knowing the set of independent eigenvectors and the eigenvalues that belong to the matrix, the matrix itself can be calculated in the following way:

$$\boldsymbol{K} = \boldsymbol{V} \boldsymbol{\alpha} \boldsymbol{V}^{-1}. \tag{16}$$

It is essential that the eigenvectors be independent; otherwise, matrix $\boldsymbol{V}$ will be singular and the calculation cannot be carried out. Fortunately, the question of singularity associated with Eq. 16 does not have severe practical consequences. Experimental eigenvalues and eigenvectors are obtained from global exponential fits to the measured data and, due to the nature of the fitting procedure, these eigenvalues are discrete. Because eigenvectors corresponding to discrete eigenvalues are independent, the experimental eigenvectors are independent. This does not, however, exclude the possibility that the kinetic scheme behind the experimental data can have degenerate solutions, i.e., multiple eigenvalues. If the degeneracy arises from a branch, the multiple eigenvalues will appear in the global exponential fit as a single apparent rate constant. The corresponding b-spectrum will then represent the sum of the multiple eigenvectors and will contain the spectral contributions of several intermediates, as in case of the simple branch discussed later. If a degeneracy of this kind is suspected, the experimental b-spectrum can be split into two or more partial b-spectra, each representing an independent eigenvector of the multiple eigenvalue. Thus, the contributions of intermediates can be separated and a degenerate kinetic scheme containing the suspected branch can be reconstructed.

Equation 16 is used to calculate the kinetic matrix. It is valid for any set of scaled eigenvectors regardless of the absolute values of the scaling factors, since the latter appear twice in the expression and in opposite senses. Notice that the amplitudes of the intermediates obtained from the decomposition of b-spectra, and corrected for the bleached components, are a set of scaled eigenvectors of the kinetic matrix. Furthermore, for the decomposition of b-spectra it is sufficient to define only the relative amplitudes of the intermediate spectra; their absolute values are not needed. Problems may, however, arise in the computation of the kinetic matrix if b-spectra are improperly decomposed, or if they do not hold sufficient information about the kinetics of the conversions in the system. In such instances the calculated kinetic matrix becomes meaningless, e.g., it will contain negative rate constants. This often indicates that the presumed components of the kinetic scheme, or their spectra used in the decomposition of b-spectra, are incorrectly defined, and further improvements are needed.

Reflections of the kinetic scheme in the shapes of b-spectra

Eigenvectors carry far more information on the interconnections in a kinetic scheme than do eigenvalues, and the experimental eigenvector matrix obtained from the decomposition of b-spectra can be regarded as the fingerprint of the reaction. In many cases the kinetic scheme, or its main elements, can be easily recognized in the shape of b-spectra. In the analysis of experimental data, especially for simplifying complex schemes, we will often refer to the connections between b-spectra compositions and combinations of steps in the kinetic scheme. Below we briefly describe the origin of a few important guidelines that we will use frequently in our further discussions.

We use a relatively simple triangle scheme connecting *A*, *B*, and *C* intermediates to demonstrate the effect of kinetic

steps on the shape of b-spectra (sample scheme below).

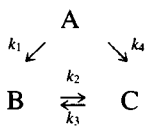

The sample scheme contains an A → B ↔ C path with reaction rate constants k_1, k_2 for the forward and k_3 for the backward steps, and an A → C branch with rate constant k_4. The kinetic matrix of this scheme is a 3 × 3 matrix, the eigenvalues and eigenvectors of which can be obtained analytically. For convenience, we will use the apparent rate constants, r_1, r_2, and r_3, which are the eigenvalues taken with negative sign:

$$r_1 = (k_1 + k_4); \quad r_2 = (k_2 + k_3); \quad r_3 = 0;$$

$$v_1 = \{1 \quad -(k_1 - k_3)/(r_1 - r_2) \quad (k_2 - k_4)/(r_1 - r_2)\};$$

$$v_2 = \left\{0 \quad \frac{k_1k_2 - k_3k_4}{r_2(r_1 - r_2)} \quad \frac{-k_1k_2 - k_3k_4}{r_2(r_1 - r_2)}\right\};$$

$$v_3 = \{0 \quad k_3/r_2 \quad k_2/r_2\}.$$

Braces are used to represent column vectors. The eigenvector columns are scaled to give {1 0 0} concentration vector at time 0. Simplified versions of this scheme represent standard step combinations frequently found in bigger and more complex schemes and will be discussed below.

1) By setting k_3 and k_4 to zero the scheme becomes a *unidirectional sequential scheme*: A → B → C. The apparent rates are equal to the microscopic rates, and when $k_1 \gg k_2$ the b-spectra are practically $A - B$ and $B - C$ difference spectra, and the time-independent b_0-spectrum is a C spectrum. We will use this type of notation for the spectral components to characterize only the qualitative composition of b-spectra without coefficients giving the actual amplitudes of the components. Notice that in each b-spectrum the major contributions come from the intermediates that participate in that step, minor contributions from intermediates of the consecutive steps, and the sign of the contributions alternates as positive/negative, etc. Intermediates that appear in earlier steps do not contribute. The latter property of the b-spectra can, in principle, be used to test the reversibility of steps. In practice, however, small contributions are not easily recognized. When k_2 is not much smaller than k_1 the first b-spectrum contains a significant positive contribution from component C and the amplitudes of B and C components in the first two b-spectra are relatively large. If k_2 exceeds k_1 we have a *slow-fast step combination*. The fastest transition shows a $C - B$ difference spectrum, the second transition shows a $A + B - C$ combination, but the b_0 is still a C spectrum. The slow-fast step combination leaves two important marks on b-spectra: it inverts the signs of the components participating in the fast step and reduces their amplitude. When analyzing experimental b-spectra of this kind the spectral shapes of b_1 and b_0 seemingly suggest that the reaction chain starts and ends with the same intermediate C. However, using the balance criteria discussed earlier, one can realize that the first intermediate must be A because both B and C appear in two b-spectra and with opposite signs, and it is A that we find only in one b-spectrum. Also, the spectral shape of the first absorption difference spectrum recorded should clearly show that A is the first intermediate, the one present at time 0.

2) Setting only k_4 to zero the general scheme becomes a *sequential scheme with back reaction*: A → B ↔ C. Now the b_0-spectrum obviously contains both B and C intermediates in a ratio determined by the equilibrium constant. If $r_1 \gg r_2$, the b_1-spectrum is not very different from the one without a back reaction; the amplitude of the b_2-spectrum, however, becomes smaller as the equilibrium shifts back to B. If $r_2 > r_1$ most of the arguments mentioned earlier for the slow-fast step combination apply with the exception of the b_2-spectrum composition. Assuming that $k_3 > k_1$, the latter will show an $A - B - C$ difference spectrum indicating that A converts to a mixture of B and C.

3) When k_2 and $k_3 = 0$ the general scheme becomes a *branched scheme*, A → B and A → C, with a kinetic matrix that has *degenerate solutions*, only one apparent rate, r_1, is different from zero. The corresponding b_1-spectrum is an $A - B - C$ difference spectrum, indicating the conversion of A into B and C simultaneously. Qualitatively, this b-spectrum is the same as the one that describes the conversion of A into a mixture of B and C, with rapid equilibrium between the latter two. The two kinetic schemes can only be distinguished if the resolution of the measurements allows the detection of the onset of the equilibrium. The b_0-spectrum contains the same B and C contributions as the b_1-spectrum, but with positive signs. The kinetic matrix describing the branched reaction cannot be calculated back from only two b-spectra. However, the kinetic matrix can be calculated in the usual manner by splitting the experimental b_0-spectrum into two individual b_0-spectra displaying the B and C components separately, and belonging to the same zero eigenvalue. This procedure can generally be applied to degenerate solutions.

4) Leaving all microscopic rates in the general scheme nonzero allows different variations in the compositions and shapes of the b-spectra. Depending on the relative values of the microscopic rates, many of the b-spectra of the general scheme, however, will resemble one of the simplified schemes discussed above, and can be approximated by one of them within experimental error.

Simplification of calculated kinetic matrices

Practical reaction schemes are usually the result of simplifications. The rates that produce contributions below the level of the experimental resolution are set to zero and the system is described by the fewest steps required to reproduce the experimental data. We will make use of this principle in sorting out the calculated kinetic schemes.

Decomposition of b-spectra into intermediate spectral components inevitably produces errors and amplitude mis-

matches, and in most cases components with very small amplitudes are completely missed. Small components in the eigenvector matrix play a large role in simplifying the calculated schemes, giving a definite direction and order in the arrangement of intermediates. The absence of small components results in the appearance of extra steps in the calculated kinetic matrix with the corresponding scheme containing branches and cross-reactions. For example, the sequential schemes discussed above require a small positive C component in their b_1-spectra when the rates are well-separated. If this component is missed in the decomposition, the calculated scheme inevitably contains a branch from A to C with a rate constant k_4 matching the value of k_2, as seen in the formulas for the eigenvectors.

Due to the limited resolution in the decomposition of b-spectra, some of the rates in the calculated kinetic matrix correspond to alternative reaction pathways leading to the formation of the same intermediate, and not all the rates are really necessary to reproduce the experimental data. This apparent drawback of the calculation method, however, can be recognized as an advantage when it is understood that the complex scheme represents the superposition of all the possible schemes. By eliminating one or the other set of extra steps, one can arrive at a number of simplified schemes that all describe the experimental data adequately. We simplify the schemes by replacing the unresolved zero components in the eigenvector matrix with small positive or negative ones and adjusting their amplitude until the extra steps disappear from the calculated scheme. This method of scheme simplification is based on the requirements of theory and is different in principle from the technique used to derive the whole kinetic scheme by eliminating some of the elements from a completely filled kinetic matrix (Nagle, 1991). In addition, we eliminate only a few extra steps from the scheme, the backbone being firmly established by the nonzero elements of the experimental eigenvector matrix. Adding the small components to the eigenvector matrix justified by theory eliminates the extra steps from the scheme without conflicting with the experimental observations. This can be confirmed by calculating and comparing the time dependencies of intermediate concentrations for the complex and the simplified schemes.

EXPERIMENTAL

Absorption difference spectra of rhodopsin were measured by an optical multichannel analyzer-based system at selected delay times in the 1-μs to 80-ms time window following a laser excitation pulse at 25°C, as described previously (Lewis et al., 1987; Hug et al., 1990). Singular-value decomposition was applied to the data matrix (Hug et al., 1990) before global exponential fitting. A minimal number of six basis spectra were used to ensure that no spectral features have been eliminated by truncation. The data showed three experimental decay constants in accordance with earlier observations, and the b-spectra had very similar shapes and amplitudes to the ones already published (Thorgeirsson et al., 1993). The b-spectra obtained here are shown in Fig. 1.

Decomposition of rhodopsin b-spectra

Spectral shapes of rhodopsin intermediates

Low-temperature absorption measurements show four intermediates in the rhodopsin photoreaction (Yoshizawa, 1972; Matthews at al., 1963), and three of them are expected to be present under our experimental conditions: lumi (497 nm), meta I (477 nm) and meta II (380 nm). The values in the parentheses refer to the position of the absorption maxima. Recent multiwavelength measurements at physiological temperatures suggested an additional intermediate absorbing at 380 nm (Thorgeirsson et al. 1992; 1993), which was named meta I-380. It appears to be isospectral with the meta II intermediate, and according to the proposed kinetic schemes it is formed earlier than meta II.

In proposing absorption spectra of the intermediates we assume that the positions of the absorption maxima may be slightly different at physiological temperatures than the ones measured at low temperatures. The spectral shapes of lumi and meta I are chosen to mimic the spectrum of rhodopsin, while meta II is deduced from the positive component of the bleached spectrum of rhodopsin. For computational purposes the spectra are represented by skewed Gaussians composed of one main band and, when appropriate, a blue-shifted broad band accounting for the absorption in the *cis*-band region. The positions of the absorption

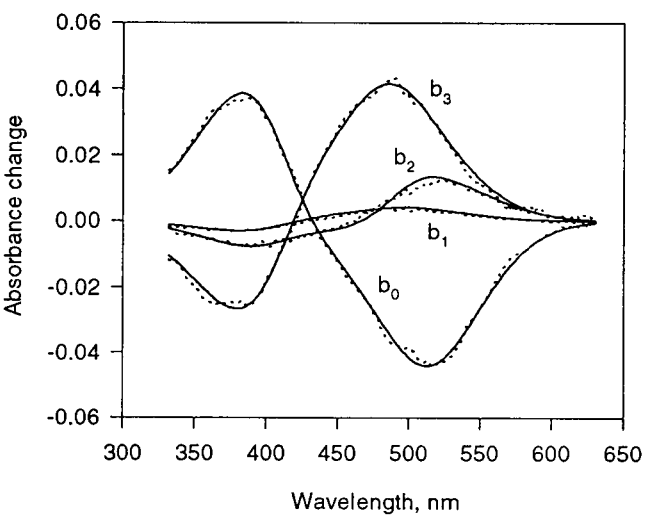

FIGURE 1 Decomposition of the experimental b-spectra into spectral components of intermediates. Dotted lines are b-spectra produced by 3-exponental global fit to the time dependence of absorption difference spectra, solid lines show the spectral sum of the intermediate components listed in Table 1 and having the shapes shown in Fig. 2. The decomposition represents the minimal number of intermediates required to reproduce the experimental b-spectra.

maxima and the relative amplitudes of the intermediate spectra can be adjusted in the computation.

Intermediate components of b-spectra

Of the four b-spectra, the b_0-spectrum can be interpreted in the most straightforward way because it has a relatively large amplitude and one component, the bleached rhodopsin spectrum, is known. In addition to a positive meta-380 and the negative rhodopsin component, the spectrum contains a small positive component in the 480 nm range, which we identify with meta I.

The b_3-spectrum has two components, a negative one in the 380-nm region and a positive one with maximum at ~480 nm that can be identified with meta I. These two components are sufficient to fit the b_3-spectrum within experimental noise.

The position and width of the positive band of the b_2-spectrum looks like a difference between two overlapping spectra. Three components are required to fit the b_2-spectrum: lumi with positive amplitude, and meta I and meta-380 with negative amplitudes.

Because of its relatively small amplitude, the composition of the b_1-spectrum is the most uncertain of the four b-spectra. It is clear that it has a negative meta-380 component but the positive band can be interpreted either as lumi, meta I, or as their mixture. Considering the large relative error in the position and amplitude of the positive peak; all three interpretations need to be evaluated together with a possible variation in the amplitudes of the intermediate components.

The spectral shapes of the intermediates, including rhodopsin, lumi, meta I and a meta-380 species used in the decomposition of the four b-spectra, were skewed Gaussians, as mentioned before. The positions of the maxima and the relative amplitudes of the spectra were adjusted until all four b-spectra were adequately fit and a rough amplitude balance was achieved. The intermediate spectra and the fit to the b-spectra are shown in Figs. 2 and 1, respectively. The amplitudes of the components, measured in mOD units, obtained from the decomposition are listed in Table 1, with the positive component of the b_1-spectrum interpreted as meta I.

The isospectral intermediate is meta I-380

The global exponential fit gives three exponentials and four b-spectra, indicating that rhodopsin bleaching is followed by four intermediate states in our experimental time window. In addition to the rhodopsin spectrum, three spectral shapes are sufficient to decompose the four b-spectra. Therefore, two of the intermediates must be isospectral within the limits of our experimental resolution.

Assuming that the fourth intermediate is isospectral with lumi or meta I is inconsistent with experimental observations for the following reasons. The amplitude of the b_1-spectrum indicates that meta II is in a fast equilibrium with lumi or meta I, or with their isospectral twins. The composition of the time-independent b_0-spectrum also shows an equilibrium in the final state, which favors the meta II intermediate. Because here we assume meta II to be the only meta-380 intermediate, the fast equilibrium must be part of the final state. The composition shown in the final state, however, cannot be reconciled with the meta II content that can be predicted from the amplitude of the b_1-spectrum. There is no contradiction between the early and the late equilibrium if there are two meta-380 components involved, an isospectral twin of meta II, the meta I-380 being present at early times.

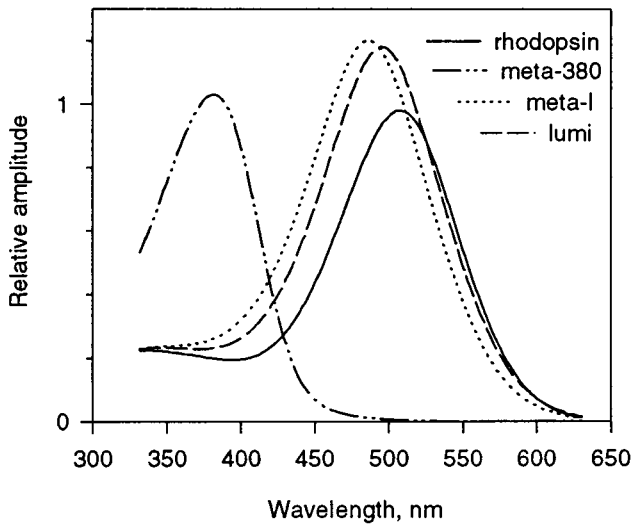

FIGURE 2 Spectral shapes of rhodopsin intermediates used in the decomposition of b-spectra. Lumi and meta I are chosen to mimic the spectrum of rhodopsin; meta-380 is deduced from the spectrum of the bleached rhodopsin. The main bands in the spectra are skewed Gaussians.

Partition of meta-380 amplitudes between meta I-380 and meta II

Although it is reasonable to assign the meta-380 component of the b_1-spectrum to meta I-380, it is not obvious how the meta-380 components of the other b-spectra should be redistributed between meta I-380 and meta II intermediates. We solve this problem in a general way. Let us assume the meta I-380 contents of b_2-, b_3-, and b_0-spectra to be a, b, and c, and the meta II contents to be a', b', and c', as shown in Table 2.

TABLE 1 Spectral components of b-spectra in mOD units and the corresponding decay time constants in seconds

	b_1	b_2	b_3	b_0
lumi	0	53.6	0	0
meta I	3.0	−46.1	35.7	11.8
meta-380	−3.2	−7.6	−34.5	45.3
rhodopsin	0	0	0	−58.0
decay time, s	6.91×10^{-5}	1.51×10^{-3}	9.51×10^{-3}	

TABLE 2 Partition of meta-380 component

	b_1	b_2	b_3	b_0
meta I-380	b_1(meta-380)	a	b	c
meta II	0	a′	b′	c′

To satisfy the balance in columns and rows, Eqs. 13 and 14, the following relations hold: $a + a' = b_2$(meta-380), $b + b' = b_3$(meta-380), and $c + c' = b_0$(meta-380); b_1(meta-380) $+ a + b + c = 0$.

Choosing b and c as variable parameters and assigning them different values, we can construct a set of 4×4 eigenvector matrices, which now represent the amplitudes of all four intermediates in the experimental b-spectra. We have to find those eigenvector matrices in this set yielding meaningful kinetic matrices.

Kinetic schemes

Specific strategy in scheme derivation for isospectral intermediates

In the absence of isospectral intermediates the general method would have been able to calculate the kinetic matrix by direct application of Eq. 16, leading to the possible kinetic schemes. However, for isospectral intermediates the decomposition of b-spectra does not yield a complete eigenvector matrix, and partitioning of components becomes necessary. Unlike the other methods of kinetic analysis, our method deals with isospectral intermediates in a straightforward way outlined below, and allows one to find all possible kinetic schemes by analyzing the partitioning of isospectral intermediates in the most general sense, introduced above.

To arrive at the final kinetic schemes we follow two guidelines: first, all possible combinations of intermediate concentrations consistent with the experimental b-spectra need to be considered; second, the kinetic scheme should contain the fewest possible steps. The first goal is achieved by exploring the field of (b, c) parameters for each interpretation of the b_1-spectrum. Using the set of eigenvector matrices and the experimental decay constants, a set of kinetic matrices can be calculated by Eq. 16. Each element in the kinetic matrix needs to be considered a function of b and c: $K_{ij}(b, c)$. Our goal is to find (b, c) pairs that give meaningful values for the elements: $K_{ii} < 0$ for the diagonal elements, and $K_{ij}(i \neq j) \geq 0$ for the elements representing the microscopic rate constants of the reaction steps, as shown in the most general scheme. The second goal is to find schemes with the simplest kinetic matrices. For this purpose we can fill in the blanks in the b_1-spectrum composition, particularly by replacing the zero value for the meta II component with a small positive or negative one. As noted in the example scheme above, the late intermediates must have nonzero amplitudes in the b-spectra; zero values result from insufficient resolution in the b-spectra decomposition because of the limitations imposed by the signal-to-noise ratio of the data. Within the limits of experimental inaccuracy we are free to add components that lead to scheme simplification. We discuss the different possible interpretations of the b_1-spectrum separately below, with the goal of simplifying the most general scheme of four intermediates shown below to those schemes consistent with experimental data.

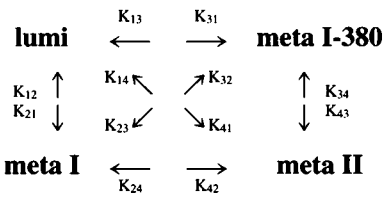

1. The b_1-spectrum contains meta I and meta I-380 components

Maximal scheme for the 3 mOD amplitude

A set of kinetic matrices was calculated in a broad range of b and c values for $b_1 = \{0\ 3\ -3.2\ 0\}$ (mOD) composition. The corresponding elements of the kinetic matrices are treated as functions of (b, c). Four matrix elements, K_{21}, K_{41}, K_{24}, and K_{34}, each representing a microscopic rate, deserve special attention because they show negative values at certain (b, c) combinations. When plotted as a function of variable b at constant c, K_{21} increases and K_{41} decreases with increasing b, and the two intercept at $b < 19$ (Fig. 3 *A*). The limit refers to the lowest possible value of c, $c = 0$. Compared with the main decay rate of lumi, K_{31}, both K_{21} and K_{41} are very small positive numbers, practically zero, at the intercept and in its vicinity. In a similar plot K_{34} increases and K_{24} decreases with increasing b for each value of c and intercept at $b > 0$ (Fig. 3 *B*). Again, the limit indicates the intercept for $c = 0$. At the intercept, K_{24} and K_{34} have positive values, therefore there is a small interval of b for each c, where both rate constants are positive.

Increasing the value of $c > 0$ shifts the intercepts of K_{21}/K_{41} and K_{24}/K_{34} in the opposite directions on the b axis. It is easy to see that for a particular $c > 0$ value, or rather an interval of it, the intercepts of the two pairs occur in the same interval of b. These common intervals of b and c for the two intercepts mentioned are centered at $b = 13$ and $c = 4.4$. When kinetic matrices are calculated for the values of b and c belonging to the common intervals, all the microscopic rate constants in the matrices are positive, and at least two of them, K_{21} and K_{41}, are zero. The nonzero positive elements of the matrix are: K_{31}, K_{32}, K_{42}, K_{23}, K_{43}, K_{24}, and K_{34}. The corresponding kinetic scheme, Scheme 1_{max}, has the maximum number of connections for this common (b, c) interval.

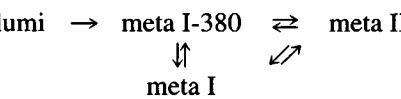

This scheme can be simplified in two ways. First, in the narrow range of possible (b, c) values we can pick those

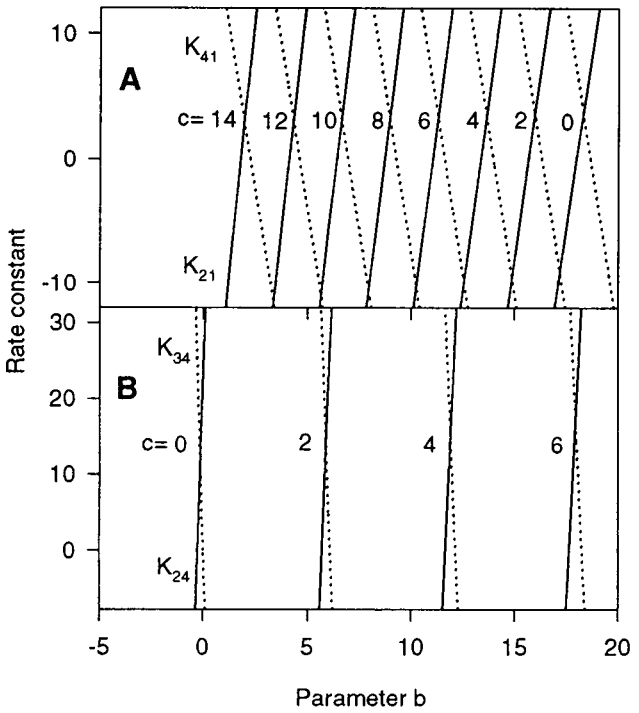

FIGURE 3 Partition of the meta-380 components of b-spectra into two isospectral components. Parameters *b* and *c* represent the amount of meta I-380 component, in mOD units, in b_3 and b_0-spectra as indicated in Table 2. Rate constants were calculated as functions of parameters *b* and *c*. Four rate constants, plotted as functions of *b* at constant *c* values, display negative values in a range of (*b*, *c*) combinations and narrow the range of the possible parameter values. The rate constants are measured in s^{-1} and correspond to the reaction rates as shown in the general scheme.

which make either K_{24} or K_{34} zero in addition to K_{21} and K_{41}. Second, we can make small adjustments to the composition of the b_1-spectrum. The b_1-spectrum must have a nonzero meta II component since meta II is at the end of all possible reaction sequences. Assigning a small positive or negative value to the b_1(meta II) component will satisfy the requirements of the theory, and can turn an additional element of the kinetic matrix into zero, and thus remove one more reaction step from the maximal scheme. The simplified schemes, Scheme 1.1 and 1.2 are discussed below.

1.1 Models with meta I ← meta II step

From the narrow range of (*b*, *c*) combinations mentioned, first we pick those that make K_{34} zero. To remove an additional reaction step we replace the zero value in b_1(meta II). Putting a small positive value does not lead to a physically meaningful scheme, a small negative value results in a linear scheme below.

Linear equilibrium model

Assigning a small negative value to b_1(meta II), b_1 = {0 3.0 −3.2 −0.021} mOD, and using (*b*, *c*) = (13.4, 4.4) mOD combination from the common interval, both K_{43} and K_{34} can be made to be zero. The corresponding eigenvector matrix yields the kinetic matrix in Table 3.

This kinetic matrix describes a sequential scheme with back reactions, Scheme 1.1.

$$\text{lumi} \rightarrow \text{meta I-380} \rightleftarrows \text{meta I} \rightleftarrows \text{meta II} \qquad \text{Scheme 1.1}$$

1.2 Models containing meta I-380 ← meta II step

Here the (*b*, *c*) combinations are selected from the common interval to remove K_{24} from the kinetic matrix and the b_1(meta II) value was adjusted to remove an additional reaction rate constant. Only a positive value in b_1(meta II) produces a physically acceptable scheme.

Branched equilibrium model, version 1

The (*b*, *c*) = (12.75, 4.36) mOD combination and a small positive meta II component in b_1, b_1 = {0 3 −3.2 0.06} mOD, removes both K_{24} and K_{42} from the calculated kinetic matrix and produces the reaction rates shown in Table 4.

The corresponding scheme is a branched equilibrium scheme, Scheme 1.2. Notice that the small positive value of b_1(meta II) removed the same reaction step, meta II to meta I, as in Scheme 1.1.

$$\begin{array}{ccccc} \text{lumi} & \rightarrow & \text{meta I-380} & \rightleftarrows & \text{meta II} \\ & & \Downarrow\Uparrow & & \\ & & \text{meta I} & & \end{array} \qquad \text{Scheme 1.2}$$

1.3. Schemes emerging for a b_1-spectrum with amplitude <3 mOD

Because the small size of the b_1-spectrum makes the relative uncertainty of its amplitude big, the 3-mOD value used in the derivation of schemes above is close to the upper limit of the possible range. We discuss the effect of smaller amplitudes on the kinetic schemes (below).

Decrease in b_1-spectrum amplitude creates shortcuts

Decreasing the amplitude of the b_1-spectrum below 3 mOD affects K_{21} and K_{41} differently. When plotted as a function of *b* at constant *c* value, the two rate constants corresponding to smaller amplitudes no longer intercept at their zero values. There is an interval of *b* for each *c* value where both rate constants are positive and no (*b*, *c*) combination allows both of them to be neglected. In a similar plot, K_{24} and K_{34}

TABLE 3 Kinetic matrix of microscopic rate constants for the linear equilibrium model

	lumi	meta I	meta I-380	meta II
lumi	−664	0	0	0
meta I	6	−3811	9998	29
meta I-380	690	3984	−10740	0
meta II	5	101	0	−29

TABLE 4 Microscopic rate constants for the branched equilibrium model, version 1

	lumi	meta I	meta I-380	meta II
lumi	−664	0	0	0
meta I	−2	−3710	10092	0
meta I-380	692	3877	−10840	31
meta II	−2	0	278	−30

intercept in the same manner as before. We evaluate the kinetic schemes for $K_{41} = 0$ and $K_{21} = 0$ separately.

1) All combinations of (*b, c*) that make K_{41}, and either K_{24} or K_{34} zero fall into a relatively narrow range: 11.5–13.5 for *b* and 3.6–4.6 for *c*. Thus, the meta I-380 and the meta II contents of the b-spectra are similar for all the different amplitudes, and the schemes differ from those discussed for the 3-mOD amplitude only by an additional step, a short cut from lumi to meta I coming from the positive K_{21}.

Scheme 1.3a

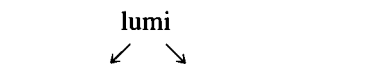

Scheme 1.3b

2) In a similar vein for each value of the b_1-spectrum amplitude there are combinations of the (*b, c*) parameters that make K_{21}, and either K_{24} or K_{34}, zero. When the amplitude drops to 1.9 mOD, both the *b* and *c* values in the combination mentioned are close to zero. Since the lower limit for *c* is zero, K_{21} cannot be made zero when the b_1-spectrum amplitude is <1.9 mOD. Because K_{41} is positive for the (*b, c*) parameters considered here, the lumi → meta II step will be present in the calculated kinetic schemes; the other steps are the ones already discussed for the 3-mOD amplitude.

Scheme 1.3c

Scheme 1.3d

The simplified schemes in 1) and 2) were derived by assigning small positive and negative values to b_1(meta II) and are extensions of the 3-mOD schemes.

Back reactions from meta I and meta II cease at a characteristic b_1 amplitude

When the amplitude of meta I in the b_1-spectrum is lowered to 1.88 mOD, both K_{21} and K_{34} are zero at (*b, c*) = (0, 0). In addition, K_{32} also becomes zero, which means that neither meta I nor meta II converts back to meta I-380. Thus, the maximal scheme for this characteristic amplitude is different from the schemes that correspond to slightly higher b_1-spectrum amplitude:

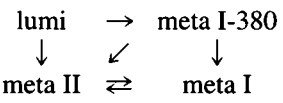

Scheme $1.3.2_{max}$

A small-positive, 0.67-mOD meta II component in b_1(meta II) eliminates the lumi-to-meta II step, which is also different from its effect at higher amplitudes where it removed the meta I-to-meta II step. The simplified kinetic scheme, Table 5, is the right-triangle scheme, version 1:

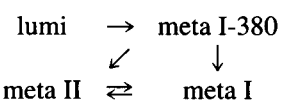

Scheme 1.3.2a

A small-negative meta II component in b_1(meta II) removes the meta I-380-to-meta II step as it does at higher amplitudes, and the resulting scheme is a square one with only one reversible step, Table 6. We will call it the inverted square model, version 1:

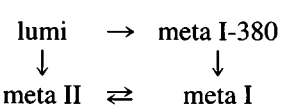

Scheme 1.3.2b

For b_1 amplitudes below 1.88 mOD only (*b, c*) = (0, 0) provides reasonable kinetic matrices, and K_{21} is no longer zero. Therefore an additional lumi-to-meta I step appears in the kinetic schemes shown above.

A special combination of parameters yields a second branched equilibrium scheme

As we have seen before, a small positive meta II component in b_1 can eliminate either K_{42}, meta I to meta II, or K_{41}, lumi to meta II, depending on the amplitude of the b_1-spectrum or the value of the (*b, c*) pair. At intermediate values of the above parameters, b_1 = {0 1.93 −2.6 0.68} and (*b, c*) = (0.7, 0.35) mOD, both of them are eliminated simultaneously and the already familiar branched equilibrium scheme, Scheme 1.2, is produced. Notice that the reaction rate constants in the kinetic matrix, Table 7, are different from the ones listed earlier for the same type of scheme. The physical meaning of the changes will be discussed later.

TABLE 5 Microscopic rate constants for the right triangle model, version 1

	lumi	meta I	meta I-380	meta II
lumi	−664	0	0	0
meta I	−2	−84	13535	22
meta I-380	515	0	−14475	0
meta II	1	81	4918	−21

TABLE 6 Microscopic rate constants for the inverted square model, version 1

	lumi	meta I	meta I-380	meta II
lumi	−664	0	0	0
meta I	−1	−84	13528	22
meta I-380	515	0	−14475	0
meta II	185	81	0	−21

TABLE 8 Kinetic matrix of microscopic rate constants for the square model

	lumi	meta I	meta I-380	meta II
lumi	−1396	0	12262	0
meta I	504	−84	1	22
meta I-380	781	0	−13743	0
meta II	0	81	3340	−21

2. The b_1-spectrum contains lumi and meta I-380 components

Maximal scheme

Here we associate the positive component in the b_1-spectrum with lumi. The first column of the eigenvector matrix contains the components of the b_1-spectrum: $b_1 = \{3\ 0\ -3.2\ 0\}$. The kinetic matrices are calculated for a set of (b, c) parameters in the same manner as before. When the matrix elements are plotted as function of b there is only a single combination, (b, c) = (0, 0) where all the rate constants are positive or zero. The kinetic matrix calculated for this combination corresponds to the scheme shown below:

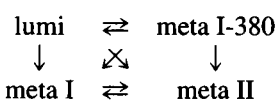

Scheme 2_{max}

The scheme has the maximal number of steps possible for this parameter and amplitude combination, and can be simplified by replacing the zero value in b_1(meta II) with a small positive or negative one. For reasons similar to those discussed above we can predict that a small positive value will eliminate the lumi-to-meta II shortcut, and a small negative value will remove the meta I-380-to-meta II step. The meaning of the small positive value is that meta II forms in the lumi → meta I-380 → meta II sequence, and not simultaneously with meta I-380, while the small negative value has the opposite meaning. Similarly, one also has to replace the zero value in b_1(meta I). A positive value of b_1(meta I) does not change the scheme. A small negative value eliminates the meta I-380-to-meta I step so that meta I forms only from lumi, in analogy with the branched example scheme discussed above.

By replacing the zero values in b_1(meta I) and b_1(meta II) we can remove two steps from the maximal scheme. The kinetic matrix calculated for $b_1 = \{3\ -0.11\ -3.2\ 0.74\}$ is in Table 8, and the scheme is the square model proposed earlier by Thorgeirsson et al. (1993):

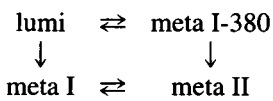

Scheme 2.a

When three components are negative in b_1, $b_1 = \{3\ -0.11\ -3.2\ -0.04\}$, all three components form simultaneously from lumi via a branched scheme. The calculated kinetic matrix is shown in Table 9. This scheme will be called the left-triangle model.

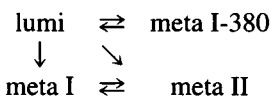

Scheme 2.b

3. The b_1-spectrum contains a mixture of lumi and meta I

Instead of analyzing the possible (b, c) combinations for the different mixtures of lumi and meta I in the b_1-spectrum, we evaluate the kinetic schemes produced by adding the missing lumi or meta I component to the b_1-spectrum in the categories discussed above.

In all situations when the meta I content is >1.88 mOD, or the b and c values are >0, introduction of lumi into the b_1-spectrum results in negative K_{12} or K_{21} rate constants in the calculated kinetic matrix. Thus the b_1-spectrum cannot be interpreted as mixture of meta I and lumi if the meta I content is >1.9 mOD. It is hard to understand at this point why this restriction applies. We will return to this problem later.

Addition of a lumi component to the b_1-spectrum having a meta I component <1.9 mOD, or when (b, c) = (0, 0), introduces an extra meta I-380-to-lumi step in the scheme, which is the K_{13} element in the calculated kinetic matrix. The larger the lumi component, the faster this back-reaction becomes. The maximal scheme for a 1.88-mOD meta I

TABLE 7 Microscopic rate constants for the branched equilibrium scheme, version 2

	lumi	meta I	meta I-380	meta II
lumi	−664	0	0	0
meta I	0	−311	10514	0
meta I-380	662	307	−14240	30
meta II	0	0	3778	−30

TABLE 9 Microscopic rate constants for the left triangle model

	lumi	meta I	meta I-380	meta II
lumi	−1396	0	12262	0
meta I	504	−84	0	22
meta I-380	781	0	−13743	0
meta II	199	81	−1	−21

content, when $(b, c) = (0, 0)$ and $K_{21} = 0$, is the following:

lumi ⇄ meta I-380
↘ ↓
meta I ⇄ meta II Scheme 3_{max}

There is only one zero component, the meta II in the b_1-spectrum, which can be adjusted to simplify the scheme. A small positive value in b_1(meta II), 0.8 mOD or $b_1 = \{1\ 1.88\ -\ 3.8\ 0.8\}$, removes the lumi to meta II step as expected and produces a kinetic matrix shown in Table 10, corresponding to a scheme which will be referred to as the right-triangle model, version 2.

lumi ⇄ meta I-380
↙ ↓
meta I ⇄ meta II Scheme 3.a

A small negative value in b_1(meta II), −0.024 mOD, or $b_1 = \{1\ 1.88\ -3\ -0.024\}$, eliminates the meta I-380-to-meta II step and leads to a square arrangement. The kinetic matrix is in Table 11, and the scheme will be called the inverted square, version 2.

lumi ⇄ meta I-380
↓ ↓
meta II ⇄ meta I Scheme 3.b

When the amplitude of meta I in the b_1-spectrum is <1.88 mOD, the rate constant of the lumi to meta I step, K_{21}, is no longer zero; it becomes a definite positive value, and this reaction step will be present in all schemes corresponding to this parameter set. The maximal scheme looks exactly like Scheme 2_{max} derived for the b_1-spectrum containing only lumi as the major positive component. The simplified schemes, however, will be different, because only one step can be removed from this scheme: either lumi-to-meta II or meta I-380-to-meta II by putting small positive or negative values in b_1(meta II). The schemes are not shown because they are extensions of the ones already presented. Note, however, that the presence of lumi in the b_1-spectrum introduces a meta I-380 to lumi step.

DISCUSSION

Reading the elements of the scheme from the eigenvector matrix

An inherent feature of our method is that once the experimental eigenvector matrix is established, the crucial elements of the scheme can be read directly from the matrix by using a few simple rules. For instance, the absence of lumi and meta I-380 in b_3 and b_0 when $(b, c) = (0, 0)$ indicates that both meta I and meta II are separated from meta I-380 and lumi by irreversible steps. The equilibrium step between meta I and meta II is a direct consequence of the b_0 composition, and the two late intermediates can form irreversibly from meta I-380 (right-triangle schemes), or from lumi (left-triangle schemes), or from both of them (square schemes).

TABLE 10 Microscopic rate constants for the right triangle model, version 2

	lumi	meta I	meta I-380	meta II
lumi	−917	0	3568	0
meta I	−1	−84	7124	22
meta I-380	961	0	−14222	0
meta II	1	81	2893	−21

TABLE 11 Microscopic rate constants for the inverted square model, version 2

	lumi	meta I	meta I-380	meta II
lumi	−917	0	4519	0
meta I	−1	−84	9018	22
meta I-380	759	0	−14222	0
meta II	197	81	1	−21

In a similar vein, the composition of the b_1-spectrum determines the fast step and its position in the scheme. When the positive component in b_1 is meta I it can mean only a slow-fast step combination because lumi is the first intermediate in the reaction sequence. A slow-fast step combination in the lumi → meta I-380 → meta I sequence can explain the small amplitude of the b_1-spectrum, and the absence of a lumi component in it. The second step in this sequence must be reversible if the late b-spectra have meta I-380 components, and irreversible if not. A number of our calculated schemes show exactly these features. The b_1-spectrum can have a lumi component, and a small amplitude at the same time, only if the lumi → meta I-380 step is reversible. This restriction applies equally to a b_1-spectrum whether it is a result of slow-fast step combination and has both lumi and meta I positive components, or it is a consequence of back-shifted equilibrium between lumi and meta I-380. These simple rules manifest themselves in all schemes, which were calculated for $(b, c) = (0, 0)$ values.

The rules can eliminate shortcuts and cross-reactions from proposed schemes. In this respect the early b-spectra are most important because they contain the characteristic component sequences that determine the whole reaction path. Each consecutive step in a sequence leaves its characteristic mark on the b-spectra. When these contributions are neglected in the decomposition of b-spectra, the calculated schemes become more complex than necessary. For example, a zero value in place of a required positive one is equivalent to compensating the positive component by a negative one of equal size, and in the calculations the zero value brings in branching in the form of shortcuts and cross-reactions. When zeros appear in place of negative values in the b-spectra composition, they act as positive values in the calculations and bring in additional sequential paths, leading to the particular intermediate via longer reaction sequences. We emphasize that adjustments to the b_1-spectrum were done to satisfy the requirements of theory and not to simplify the kinetic matrix. However, the actual values were chosen in such a way that certain steps could be

eliminated from the scheme. This provides a way to generate a number of possible simplified schemes that need to be tested with additional experimental evidence.

Limitations on the lumi and meta I mixture in the b_1-spectrum are related to reversibility of the lumi-to-meta I-380 reaction step

The analysis of schemes derived for b_1-spectra with significant lumi content showed that the presence of lumi introduces a back reaction from meta I-380 to lumi. This was true even when meta I was not present in the b_1-spectrum. The physical reason behind the reversible step was explained in the previous paragraph. The peculiar observation that no lumi can be introduced into any of the b_1-spectra when $(b, c) > (0, 0)$ or when the meta I-380 component is >1.9 mOD is connected to the appearance of this back reaction. Under those conditions meta I-380, meta I, and meta II would be interconnected via reversible steps. The presence of lumi in the b_1-spectrum would mean an additional reversible step between lumi and meta I-380, i.e., all four components would be connected via reversible steps. The latter would require the presence of lumi in all b-spectra, and none is in b_3 and b_0. The restriction is therefore caused by the limitations of b-spectra decomposition and can only be lifted by improving the resolution of the decomposition, which, obviously, requires higher quality experimental data. The simplest way to test whether a back-reaction step between lumi and meta I-380 is required in one or the other particular reaction scheme under certain conditions would be to introduce it into the kinetic matrix and refine the rate constants in the scheme by obtaining the best fit to the b-spectra.

Two versions of the branched equilibrium scheme

An interesting aspect of the branched equilibrium scheme is that it can have two sets of microscopic rate constants. A close examination of the corresponding kinetic matrices reveals that only two steps are significantly different in the two versions: meta I to meta I-380 and meta I-380 to meta II; the rest are basically the same. Furthermore, the values of the rate constants of these steps are switched in the two versions. In version 1 the meta I-to-meta I-380 step is faster than the meta I-380-to-meta II; in version 2, just the opposite.

It is easy to visualize why the two versions are equivalent as far as the overall spectral changes are concerned. The reaction steps in question produce meta I-380 and meta II intermediates, respectively, and because they are isospectral the spectral change will be indifferent to switching the two rates. Take, for instance, the spectral change represented by the b_2-spectrum. In version 1 lumi converts into a mixture of meta I and meta I-380, which are in fast equilibrium. A significant amount of meta I-380 is present because the rate of the meta I-to-meta I-380 back-reaction is relatively large. Inasmuch as meta II is formed slowly from meta I-380, its contribution to the b_2-spectrum is positive, as expected for a normal sequence of steps. In version 2, meta II is formed from meta I-380, simultaneously with the fast meta I formation, and lumi converts into a mixture of three components in fast equilibrium, which favors meta I and meta II. The net result in both versions is the formation of an intermediate, which absorbs in the 380-nm region. The overall spectral changes represented by the other b-spectra can be interpreted in a similar way.

The equivalency of the apparent rates for the two versions can also be easily visualized for the first and second rates, but the third one is too complex to deal with in a simple way. Take, for instance, the fastest apparent rate, which is largely determined by the rate of the meta I-380-to-meta I step. In version 1 this step and the meta I-to-meta I-380 step are part of a reversible reaction, and the onset of the equilibrium is determined by the sum of the two microscopic rates. In version 2 the second fastest step is the meta I-380-to-meta II conversion. The two fastest steps are part of the branched decay of meta I-380, and again the apparent rate includes the sum of the two microscopic rates.

Although the overall spectral change is the same for the two versions of the branched equilibrium scheme, the time dependencies of meta I-380 and meta II concentrations are clearly different (Fig. 4). In version 1 there is a significant amount of meta I-380 present in the final equilibrium, while in version 2 the final 380-nm component is predominantly meta II. The protonation state of the Schiff's base in the two intermediates is the same, and it is believed that they differ in the conformation of the protein (Thorgeirsson et al., 1992). The landscape of the reaction energy surface, which determines the kinetics and the activation parameters, and the physical state of the final products for the two versions, are different. This should provide clues to distinguish between them by physical means.

General characterization of the new method

In our approach toward solving the underdetermined kinetic problem we started from the same position as one of the traditional methods, namely by making assumptions about the spectra of the intermediates. By doing so we used not only the available information from other sources regarding the spectral shapes of the intermediates, but also the spectral information from b-spectra, combined with the limitations imposed by the balance equations of the eigenvector matrix. We have every reason to believe that our intermediate spectra are reasonably accurate, as confirmed by the good agreement between the assumed intermediate spectra and those calculated using the kinetic matrix determined from the data.

It is interesting to see the kind of results produced by the traditional method applied to our experimental data. Using the intermediate spectra, we derived the time-dependence of

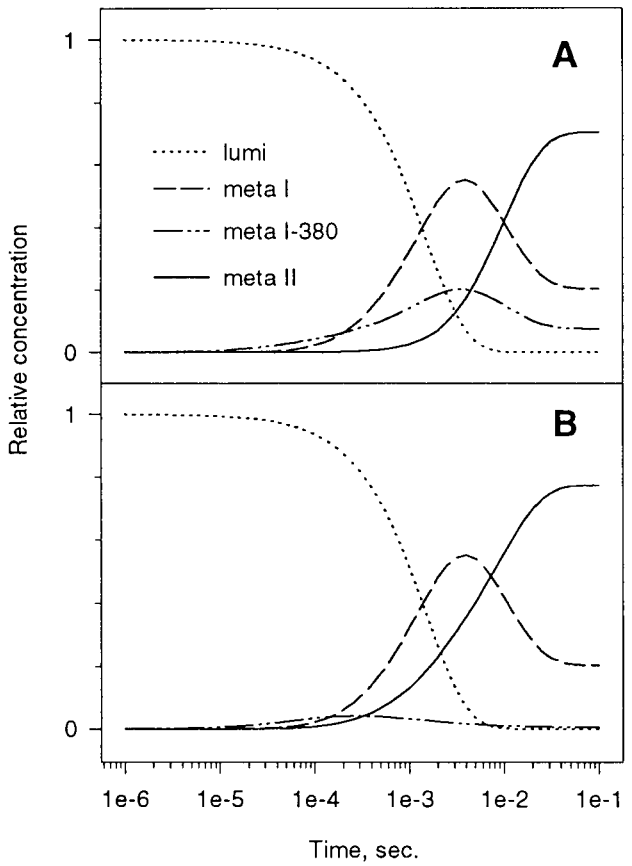

FIGURE 4 Time dependence of the relative concentrations of intermediates for the two versions of the branched equilibrium model. The versions represent two different partitions of the meta-380 component from the experimental b-spectra into isospectral meta I-380 and meta II components. Version 1 (*A*) was calculated from the kinetic matrix in Table 4, and version 2 (*B*) from the data in Table 7. The time courses of the meta I-380 concentrations predicted by the two versions are significantly different.

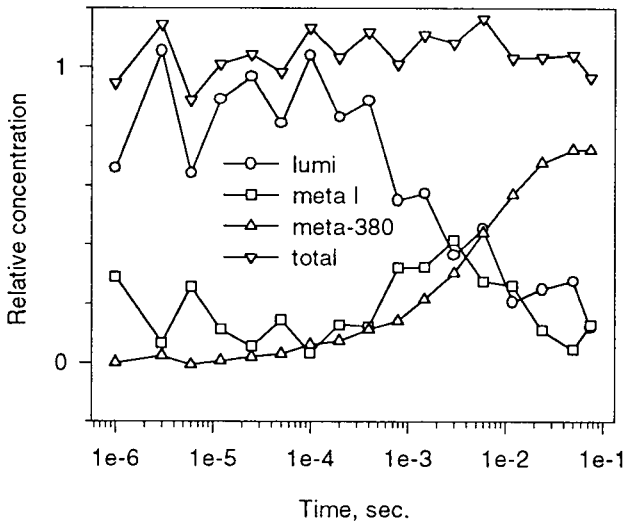

FIGURE 5 Classical approach applied to the time-dependent absorption difference spectra: the time dependence of the relative concentrations of the spectrally different intermediate forms. Intermediate concentrations at different time delays were calculated from the absorption spectra and the presumed intermediate spectra shown in Fig. 2. Data points represent the compositions from the best fit to the absorption spectra corrected for the bleached rhodopsin spectrum. The contributions of lumi and meta I can only be separated poorly in the individual spectra. Therefore the compositions at adjacent time delays do not follow a smooth trend (compare with Fig. 4).

the concentration vector from the experimental absorption difference spectra. While the sum of the intermediate concentrations is reasonably constant and equal to the theoretical value, a criterion often used to judge the quality of the decomposition in time (Nagle et al., 1995), the individual concentration curves are not very promising. As seen in Fig. 5, the adjacent data points are sometimes decomposed into dissimilar compositions, which are physically meaningless. The concentration profiles could hardly be used for analysis without correcting their shape, which would inevitably bias the possible schemes. Comparison of Figs. 4 and 5 shows a clear advantage of the current method of analysis.

The biggest problem with the traditional analysis, however, is not the accuracy of the data, but the isospectral character of two intermediates, both absorbing in the 380-nm region. Because of this there is only one concentration profile for the two, and obviously it is the sum of the two concentrations. Traditionally there is no criterion to separate them. Thus we cannot use the information given by the time-dependence of the concentrations of the meta-380 intermediate pair to propose kinetic schemes, and the search for the scheme becomes predominantly ad hoc.

One of the advantages of our method is the capacity to deal with isospectral intermediates. The procedure is based on firm theoretical ground and will produce a complete set of solutions in the form of kinetic schemes that all satisfy the experimental data within the limits of resolution. A fitting procedure shows that these solutions all represent parameter sets of local minima with practically the same depths. Besides providing this complete set of possible mechanisms, our method was able to derive two sets of parameters for the branched equilibrium model. This explains the previous observation that the simplex fitting procedure, when it was applied to optimize the microscopic rate constants in the proposed kinetic matrix, was not always able to find the proper rate constants, i.e., that followed the Arrhenius law, for this scheme (Thorgeirsson et al. 1993). This type of complete exploration of possible mechanisms and parameterizations is impossible to achieve using an ad hoc selection method.

We should mention a few practical limitations of the method. It is expected that for more than two isospectral intermediates there will be major analytical difficulties in finding the possible schemes. The decomposition of b-spectra becomes difficult for large numbers of intermediates, especially when the apparent rates are not sufficiently separated and/or the spectral forms of the intermediates substantially overlap.

CONCLUSION

We introduced a novel mathematical treatment in the kinetic analysis of time-dependent absorption data that is based on algebraic methods and allows the calculation of possible kinetic schemes. With our approach the problems associated with isospectral intermediates can be overcome and the kinetics can be successfully solved. This approach allows us to determine all possible reaction schemes that are consistent with available time-resolved spectral data. Applying this method to the time-resolved absorption data obtained at 25°C upon photolysis of rhodopsin shows that a number of mechanisms can be consistent with these data, including linear schemes with equilibrium steps, branched mechanisms, and square reaction paths. To distinguish the true mechanism from this group of possible mechanisms requires further experimental data, such as the changes in kinetics observed at different temperatures or at different pH. Such analysis will be presented in a future publication.

This work was supported by Grant EY00983 from the National Eye Institute of the National Institutes of Health.

REFERENCES

Chen, E., V. N. Lapko, J. W. Lewis, P.-S. Song, and D. S. Kliger. 1996. Mechanism of native oat phytochrome photoreversion: a time-resolved absorption investigation. *Biochemistry.* 35:843–850.

Henry, E. R. 1997. The use of matrix methods in the modeling of spectroscopic data sets. *Biophys. J.* 72:652–673.

Hofmann, K. P. 1986. Photoproducts of rhodopsin in the disc membrane. *Photobiochem. Photobiophys.* 13:309–327.

Hofrichter, J., J. H. Sommer, E. R. Henry, and W. A. Eaton. 1983. Nanosecond absorption spectroscopy of hemoglobin: elementary processes in kinetic cooperativity. *Proc. Natl. Acad. Sci. USA.* 80: 2235–2239.

Hug, S. J., J. W. Lewis, C. M. Einterz, T. E. Thorgeirsson, and D. S. Kliger. 1990. Nanosecond photolysis of rhodopsin: evidence for a new, blue-shifted intermediate. *Biochemistry.* 29:1475–1485.

Lewis, J. W., J. Warner, C. M. Einterz, and D. S. Kliger. 1987. Noise reduction in laser photolysis studies of photolable samples using an optical multichannel analyzer. *Rev. Sci. Instrum.* 58:945–949.

Linschitz, H., and V. Kasche. 1966. The kinetics of phytochrome conversion. *J. Biol. Chem.* 241:3395–3403.

Lozier, R. H., A. Xie, J. Hofrichter, and G. M. Clore. 1992. Reversible steps in the bacteriorhodopsin photocycle. *Proc. Acad. Sci. USA.* 89: 3610–3614.

Matthews, R. G., R. Hubbard, P. K. Brown, and G. Wald. 1963. Tautomeric forms of metarhodopsin. *J. Gen. Physiol.* 47:215–240.

Nagle, J. F. 1991. Solving complex photocycle kinetics. Theory and direct method. *Biophys. J.* 59:476–487.

Nagle, J. F., L. Zimanyi, and J. K. Lanyi. 1995. Testing bR photocycle kinetics. *Biophys. J.* 68:1490–1499.

Parkhurst, L. J. 1979. Hemoglobin and myoglobin ligand kinetics. *Ann. Rev. Phys. Chem.* 30:503–546.

Straume, M., D. C. Mitchell, J. L. Miller, and B. J. Litman. 1990. Interconversion of metarhodopsins I and II: a branched photointermediate decay model. *Biochemistry.* 29:9135–9142.

Thorgeirsson, T. E., J. W. Lewis, S. E. Wallace-Williams, and D. S. Kliger. 1992. Photolysis of rhodopsin results in deprotonation of its retinal Schiff's base prior to formation of metarhodopsin. II. *Photochem. Photobiol.* 56:1135–1144.

Thorgeirsson, T. E., J. W. Lewis, S. E. Wallace-Williams, and D. S. Kliger. 1993. Effects of temperature on rhodopsin photointermediates from lumirhodopsin to metarhodopsin. II. *Biochemistry.* 32:13861–13872.

Varo, G., and J. K. Lanyi. 1991. Kinetic and spectroscopic evidence for an irreversible step between deprotonation and reprotonation of the Schiff base in the bacteriorhodopsin photocycle. *Biochemistry.* 30:5008–5015.

Yoshizawa, T. 1972. The behaviour of visual pigments at low temperatures. *In* Handbook of Sensory Physiology, Vol. 7, H. J. A. Dartnall, editor. Springer-Verlag, Berlin. 145–179.